applied sciences

MDPI

Article

Investigation of Lateral and Longitudinal Deformation of Submarine Nuclear Power Plant Water-Intake Tunnel on Non-Uniform Soft Soil during Earthquake

Jie Zhao [1,*], Bo Qian [1], Changjiang Gan [2], Jianshan Wang [1] and Yanli Peng [1]

[1] School of Architectural Engineering, Dalian University, Dalian 116622, China; qian_jingbo@163.com (B.Q.); 13970381575@163.com (J.W.); 18783535782@163.com (Y.P.)
[2] Gansu Comprehensive Railway Engineering Contracting Co., Ltd., Lanzhou 730030, China; gan420210@163.com
* Correspondence: zhaojie_gd@163.com

Abstract: The safety-grade water-intake immersed tunnel plays a vital role in the nuclear power cooling system, and its seismic safety is crucial. This paper employs the response displacement method and dynamic time-history analysis using the finite element software ANSYS to construct a beam–spring model and a 3D finite element model of a shield tunnel and foundation. It also develops equivalent linear dynamic constitutive and viscoelastic boundary element subprograms. This study focuses on the weak joint sections of immersed tunnels, conducting a seismic performance analysis under extreme safety earthquake conditions (SL-2). The results indicate that the joint stiffness of immersed tunnels and the increase in seismic peak values do not affect the trend of joint opening variation with longitudinal position. The change in joint opening is primarily located where the thickness of the cover layer changes abruptly or where the soil hardness is unevenly distributed. The joint opening is mainly influenced by seismic forces when considering static and dynamic superposition. When the stiffness of the joint GINA water stop exceeds a certain value, the correlation between stiffness change and joint compression–tension variation gradually weakens. This research can provide a reference for the seismic design of similar projects.

Keywords: immersed tunnels; seismic analysis; response displacement method; time-history analysis method; joint opening

Citation: Zhao, J.; Qian, B.; Gan, C.; Wang, J.; Peng, Y. Investigation of Lateral and Longitudinal Deformation of Submarine Nuclear Power Plant Water-Intake Tunnel on Non-Uniform Soft Soil during Earthquake. *Appl. Sci.* **2024**, *14*, 5565. https://doi.org/10.3390/app14135565

Academic Editor: Roberto Zivieri

Received: 7 May 2024
Revised: 15 June 2024
Accepted: 16 June 2024
Published: 26 June 2024

1. Introduction

In recent years, China's intensified investment in new energy construction has spurred the rapid development of nuclear power as a viable alternative. Currently, most nuclear power plants in China are situated in coastal areas, utilizing seawater once-through cooling systems that require substantial water intake. Immersed tunnels are widely employed in these systems due to their minimal sea surface area requirements, eco-friendliness, cost efficiency, and straightforward construction. Given China's susceptibility to earthquakes, many plant sites are located in regions with high seismic activity. Earthquakes present a significant threat to the safety of nuclear power facilities, making seismic performance a critical concern in the construction of these projects. Currently, a well-developed research system exists for seismic studies in underground engineering. Seismic response data have been analyzed using scaled-down tunnel models designed for indoor shaking table tests. Yan et al. [1] proposed a design method for a compartmental particle damper suitable for immersed tunnels. They constructed a 1:60 scale model of an immersed tunnel and performed shaking table tests before and after installing the particle dampers. Cheng et al. [2] based their research on the Hong Kong–Zhuhai–Macao Bridge immersed tunnel project, conducting shaking table model tests on immersed tunnel systems under three site conditions (dry sand, saturated sand, and underwater saturated sand) with models

at a 1:30 scale ratio. Zhang et al. [3] investigated the dynamic response characteristics of immersed tunnel structures and their joints using shaking table tests, considering longitudinal traveling wave excitation with varying apparent velocities. Yuan et al. [4] performed compression–shear tests on joints at a 1:10 geometric scale, examining their mechanical properties under low cyclic loading. Okamoto et al. [5] conducted underwater shaking table tests on small-scale immersed tunnel models to measure seismic response data. Chen et al. [6], through shaking table tests, explored the effect of unsaturated soil foundations on internal force distribution in immersed tunnels. Yang et al. [7] analyzed the displacement behavior of immersed tunnels under seismic activity, providing valuable references for seismic studies. Li et al. [8] performed shaking table tests under multi-dimensional seismic waves, focusing on the tunnel–soil system to study the dynamic response of tunnels and surrounding soil. With the continuous advancement of finite element method theory and computer technology, numerical simulation has become a prevalent and cost-effective method for studying the dynamic responses of underwater structures. Peng [9] developed a mechanical model to examine the interaction between immersed tunnels, soil, and fluid. Using the Newmark algorithm, he investigated stress changes in immersed tunnel structures under various seismic excitations and water depth conditions. Chen et al. [10] considered the dynamic nonlinear properties of seabed soil and tunnel concrete, along with the coupling effects between seawater and the seabed, developing a finite element model to analyze the interactions among seawater, seabed, and tunnel, focusing on the seismic response of undersea tunnels. Cui et al. [11] utilized finite element software ADINA to create an integrated model of seawater, immersed tunnels, and the seabed, analyzing the seismic responses of immersed tunnel structures under various conditions, specifically with vertically incident seismic P-waves.

Immersed tunnels, characterized by long linear structures with numerous joints, are often situated in complex marine environments. These joints, critical components connecting tunnel segments, possess significantly lower stiffness than the precast concrete segments. During seismic activities or uneven foundation settlement, the joints are subjected to considerable shear forces, necessitating the design of shear keys to resist these forces. The joints often represent the most vulnerable points in the structure, enduring substantial stress and requiring special attention in seismic analysis to ensure the tunnel's overall integrity and safety. Xiao et al. [12] employed a piecewise linear method to address the material nonlinearities of the joints, investigating their response under quasi-static loads through three-dimensional refined modeling. Zhang et al. [13] used a simplified model of nonlinear spring elements for immersed tunnel joints, complemented by three-dimensional finite element modeling for seismic analysis, enabling calculations of deformation and internal force responses under seismic loading. Yu et al. [14] developed a multi-scale seismic response analysis model, exploring characteristics such as stress on tunnel segments, joint deformation, and shear key forces, along with the influence of key factors. He et al. [15] used the finite element method combined with visco-spring artificial boundaries to formulate a three-dimensional planar SV wave incidence method, investigating the mechanical properties of shear keys in the Hong Kong–Zhuhai–Macao Bridge immersed tunnel joints. Cui et al. [16] combined shaking table tests and finite element simulations to examine the impact of tunnel joints and overlying water on the seismic response of immersed tunnels. Bai et al. [17] used ABAQUS finite element software to create a three-dimensional model for seismic dynamic analysis of part of the Hong Kong–Zhuhai–Macao Bridge immersed tunnel project. Immersed tunnels on the seabed frequently experience significant internal forces due to temperature-induced loads and uneven foundation settlement. Excessive internal forces can lead to joint cracks, leakage, and, in severe cases, misalignment of the joints. To mitigate leakage and accommodate deformations in complex environments, adding water stops at the joint areas is essential [18–20]. The most widely used water stops are the GINA and OMEGA types. The GINA water stop is primarily utilized for anti-deformation and waterproofing functions, while the OMEGA water stop [21–23], acting as a secondary defense line, connects immersed tunnels, providing additional waterproofing

and effectively addressing deformations due to temperature and water pressure, concrete shrinkage, and stratum movements. Liu et al. [24] determined the minimum compression necessary to ensure the watertightness of GINA water stops using the average water pressure method and the contact stress method, establishing a safety warning level based on the remaining compression. Zhang et al. [25] investigated the material properties of GINA rubber water stops, the force and deformation mechanisms of vertical steel shear keys in joints under shear forces, and the impact of different axial water pressures on the vertical shear characteristics of the joints.

Given that China's undersea tunnels have not yet undergone strong seismic testing, the seismic stability of underwater immersed tunnels under ultimate seismic ground motion (SL-2) presents a significant technical challenge and key issue for seawater-intake projects at coastal nuclear power plants. This study focuses on the Changjiang Nuclear Power Units 3 and 4's discharge immersed tunnel project in Hainan. Utilizing the response displacement method and the time-history analysis method, the finite element software ANSYS (15.0) [26] was employed to conduct a seismic performance analysis of the safety level of seawater-intake immersed tunnels. This study involved establishing transverse and longitudinal beam–spring models and a three-dimensional soil–structure finite element model. Our research highlights the distribution of interlayer displacement within the immersed tunnel sections under seismic conditions, investigates the variations in compression–tension of GINA water stops and joint openings, and analyzes the primary factors affecting maximum deformation.

2. Methods and Principles

2.1. Response Displacement Method

2.1.1. Lateral Response Deformation Method

The reaction displacement method is applicable for performing seismic analysis of underground pipe culverts. During the analysis, the interaction between soil layers and the tunnel is modeled by arranging stratum springs around the immersed tunnel. Meanwhile, the seismic load is imparted to the structure through the foundation springs, as illustrated in Figure 1.

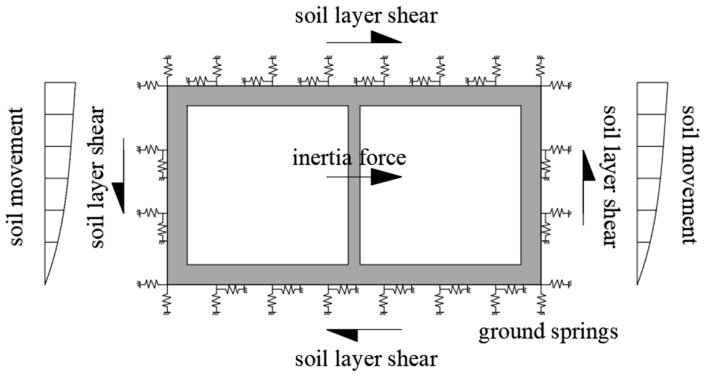

Figure 1. Calculation diagram of response displacement method.

2.1.2. Longitudinal Response Displacement Method

In this study, a beam–spring combined model is utilized to simulate the precast immersed tunnel segments and the surrounding soil. Precast immersed tunnels are modeled with beam elements, while the joint areas of the immersed tunnels are represented using spring elements. In this model, each node is equipped with soil springs in two directions, axial and transverse, along the tunnel axis to simulate the foundation soil layers, thereby forming a system for the analysis of the immersed tunnel–joint–foundation, as illustrated in Figure 2.

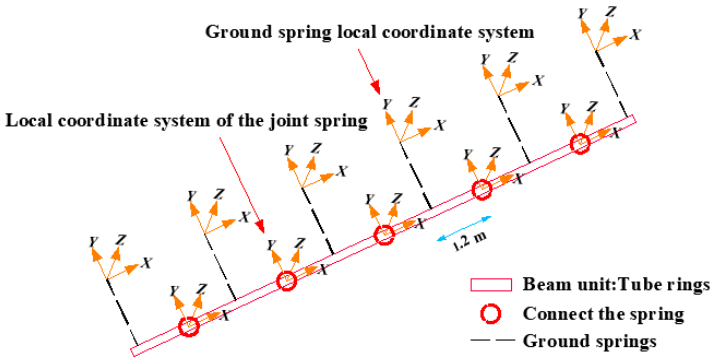

Figure 2. Longitudinal seismic response analysis model.

Utilizing the theories mentioned above, this study employs SuperFLUSH/2D (ver 6.0) software to perform free-field nonlinear dynamical analysis, thereby obtaining the relative displacements of the surrounding soil under seismic conditions. These displacements are subsequently applied as static loads to the restrained ends of the ground springs at the responsive segments of the analysis model for calculation.

2.2. Equivalent Linear Dynamic Time-History Analysis Method

The "Standard for Seismic Design of Nuclear Power Plants" in China [27] and the American ASCE 4-98 [28] advocate for the use of an equivalent linearization technique to characterize the nonlinear characteristics of non-rock foundations. By transforming nonlinear issues into linear problems, this approach greatly improves computational efficiency and is extensively used in the seismic analysis of nuclear power structures. Cao et al. [29] verified the feasibility of the equivalent linear method in finite element software using ANSYS's secondary development function. The key to applying the equivalent linearization technique is the calculation of the effective shear strain of the soil. First, an analysis is performed with a predefined initial effective shear strain derived from material characteristics. Subsequently, the new soil equivalent shear modulus and damping ratio are calculated from the G-γ and D-γ curves. This specific calculation process is delineated in Figure 3. In the plot, D represents the damping ratio, G represents the dynamic shear modulus ratio, and γ represents the equivalent shear strain. Based on practical engineering experience, generally, three to five iterations are typically sufficient to achieve satisfactory convergence results.

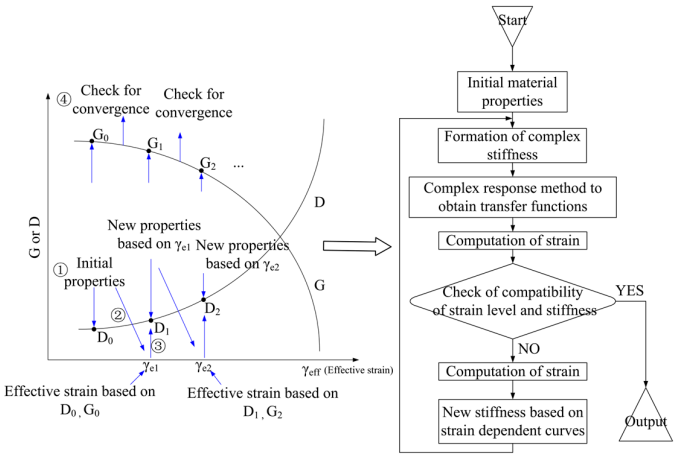

Figure 3. Schematic diagram of equivalent linear method.

2.2.1. Viscoelastic Artificial Boundary

The consideration of dynamic artificial boundaries is a key aspect in the study of the seismic performance of underwater immersed tunnels. The fundamental principle of the

viscoelastic artificial boundary involves creating a new physical element by combining dampers and springs in parallel, which can be positioned at the foundation boundary to simulate the radiation damping effect of a semi-infinite foundation. The seismic waves encountered at the model boundaries are transformed into equivalent loads for each node at the boundary. When the scattered waves propagating towards the boundary are absorbed by the viscoelastic artificial boundary, the respective nodes at the boundary will exhibit free-field motion in response to the seismic load. A schematic diagram illustrating the boundary conditions is presented in Figure 4. In order to facilitate the analysis of three-dimensional seismic responses of complex structures such as submarine immersed tube tunnels, a secondary development based on Fortran was carried out using the UPFs provided by ANSYS. This involved writing a subroutine for equivalent viscoelastic boundary elements embedded in the software. The tangential and normal spring stiffness, denoted as K, and damping coefficient, denoted as C, are calculated using Equations (1) and (2) [30], respectively.

$$K = \alpha \frac{G}{r} \sum_{i=1}^{I} A_i \quad (1)$$

$$C = \rho c \sum_{i=1}^{I} A_i \quad (2)$$

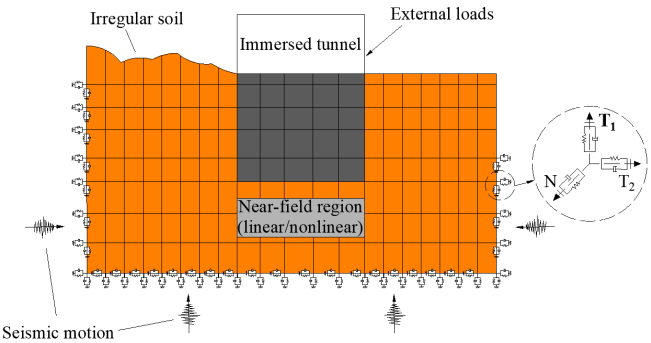

Figure 4. Schematic diagram of artificial boundary model.

In the formula, G represents the shear modulus, ρ denotes the mass density, r is the distance from the scattering source to the nodes on the artificial boundary, and c is the wave speed. The parameter α stands for the boundary parameters of different directional boundaries, while A represents the control area of the nodes at the outer boundary of the foundation region.

2.2.2. Hydrodynamic Pressure

It is widely acknowledged that seismic activity significantly influences the hydrodynamic pressure on the water-intake pipe culverts of nuclear power plants, markedly affecting the structure's dynamic response. Consequently, this pressure is a crucial dynamic load in the design of water-intake tunnels. Relevant regulations are specified in American standards (ASCE 4-98) [28]. In seismic response analysis, it is essential to consider both convective and impulsive effects arising from the oscillation of water flow within the immersed tunnel due to seismic activity. This oscillation induces pressure on the tunnel walls, necessitating the consideration of both horizontal and vertical components of fluid motion. The Housner spring–mass system [31], used to calculate hydrodynamic pressure, is illustrated in Figure 5.

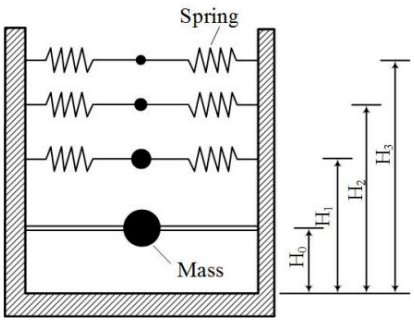

Figure 5. Housner system for hydrodynamic pressure.

3. Engineering Example

3.1. Project Parameters

The Changjiang Nuclear Power Plant, situated in Changjiang County, Hainan Province, features precast drainage immersed tunnels that extend for a total length of 3798.5 m, with a single-hole cross-sectional dimension of 6.0 × 6.0 m. Each tunnel segment measures 45 m in length, with the middle partition walls having a thickness of 40 cm and the remaining partition walls being 60 cm thick. The top of the immersed tunnels is overlaid with a rock layer at least 1.5 m thick. The tube's bottom features a fully paved crushed-stone foundation. The cross-section of the immersed tunnels is depicted in Figure 6. The tubes are connected via a flat joining method. At the joints between each pair of tunnel sections, GINA water stops are arranged around the outer wall and the mid-partition wall.

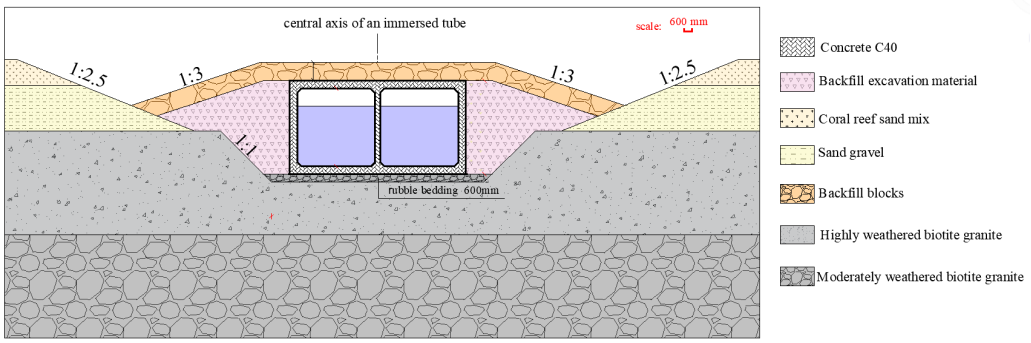

Figure 6. Cross-section view of immersed tunnel.

3.1.1. Soil Parameters

According to the geotechnical engineering survey report for the Changjiang Nuclear Power Plant site in Hainan, the site's strata primarily consist of intrusive rocks and the Quaternary system. The Quaternary system, predominantly distributed across the coastal plains and plateau geomorphic units of the plant area, mainly comprises marine and residual deposits, with a maximum thickness of 41.20 m as revealed by this survey. The site's intrusive rocks predominantly consist of biotite granite. Existing geological data indicate the presence of small areas of lamprophyre, granite porphyry, and other vein rocks. However, due to their limited distribution and minimal impact on the foundation, these formations are not considered in this study. For research convenience, rock bodies sharing similar mechanical properties and indistinct boundaries are amalgamated into a single layer.

By considering the submerged tunnel and stiffer rock foundation as elastic materials, the physical parameters are presented in Table 1. The remaining soil materials must account for their nonlinear characteristics, and the aforementioned equivalent linear method is utilized for dynamic analysis calculations. The necessary equivalent linear parameters are illustrated in Figure 7.

Table 1. Immersed tunnel and soil material parameters.

Material	Static Elastic Modulus (E/GPa)	Dynamic Elastic Modulus (E_d/GPa)	Poisson Ratio (μ)	Dynamic Poisson Ratio (μ_d)
Concrete C40	32.50	42.25	0.20	0.20
Backfill blocks	0.26	0.52	0.33	0.45
Backfill excavation material	0.26	0.52	0.33	0.45
Moderately weathered biotite granite	34.10	16.80	0.20	0.34

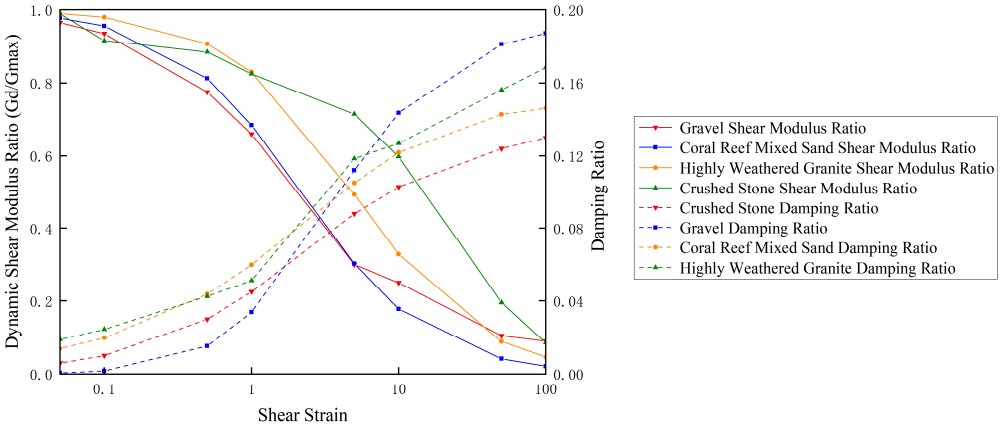

Figure 7. Dynamic shear modulus ratio and damping ratio of soil samples.

3.1.2. Seismic Parameters

This seismic analysis is based on seismic waves originating from the Changjiang Nuclear Power Plant site in Hainan. Figure 8 depicts the seismic waves and frequency spectra in three dimensions. Considering the SL-2 limit for safety seismic motion, the peak accelerations are 0.3 g in the X and Y directions and 0.2 g in the Z direction. This seismic wave lasts for 30 s, with significant fluctuations occurring between 3 and 14 s. The peak times in these directions occur at 13.59 s, 11.67 s, and 6.13 s, respectively.

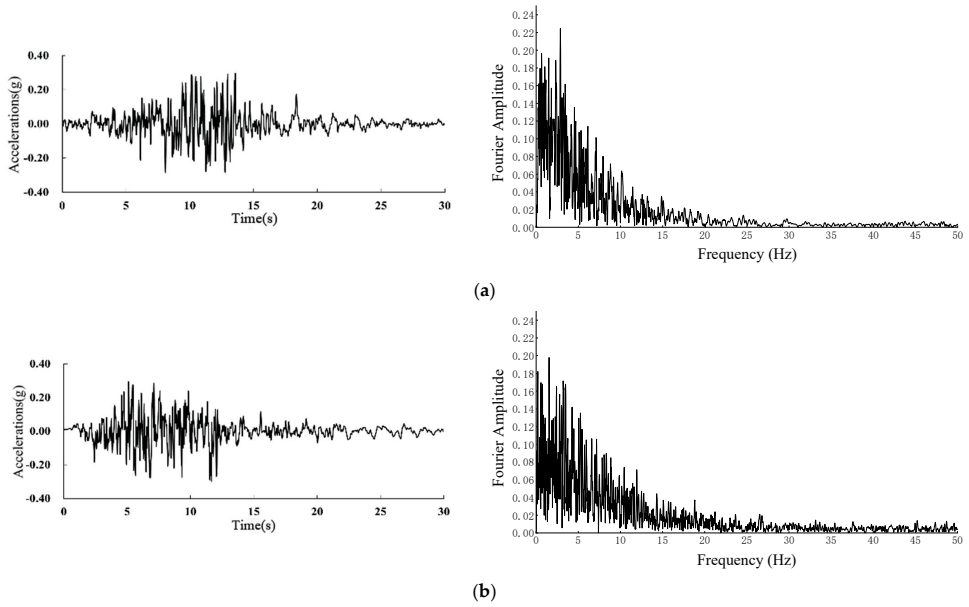

Figure 8. *Cont.*

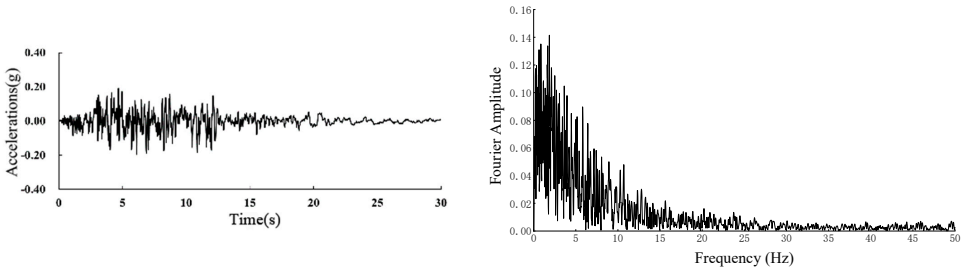

(**c**)

Figure 8. Time-history curve of seismic wave: (**a**) X-direction seismic wave and frequency spectrum; (**b**) Y-direction seismic wave and frequency spectrum; (**c**) Z-direction seismic wave and frequency spectrum.

3.2. Numerical Analysis Based on the Response Displacement Method

Due to the relative weakness of joint areas compared to the strength of immersed sections, seismic damage generally initiates at the joints. Compared to highway and railway tunnels, analyzing the seismic control indicators for the joints of nuclear power plant water-intake immersed tunnels, which demand higher water tightness, is particularly important. In this section, based on the response displacement method, a beam–spring model is established to study the interlayer displacement angle and joint opening under extreme seismic conditions in immersed tunnels.

3.2.1. Calculation Model

(1) Lateral Model of Immersed Tunnel

In order to study the stability of each wall of the immersed tunnel under earthquake conditions, the beam element (BEAM188) is used to simulate its walls, while the spring element (COMBIN14) is adopted to simulate the effect of surrounding soil on the tunnel's structure. Based on this, the lateral seismic response model is established, as shown in Figure 9.

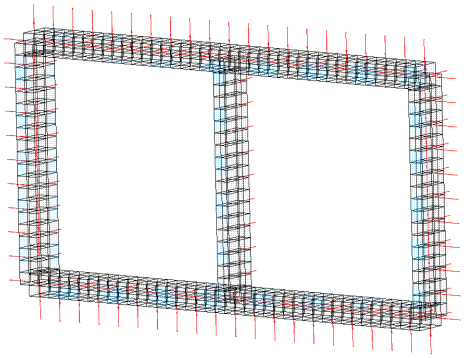

Figure 9. Transverse beam–spring model.

(2) Longitudinal Analysis Model of Immersed Tunnel

To investigate the deformation patterns of joints in the immersed tunnel under seismic conditions, 46 segments of the immersed tube in a representative sea area are selected for analysis, with a total length of 2070 m. The beam element (BEAM188) is chosen to simulate the immersed tunnel joints, while the spring element (COMBIN14) is used to simulate the rotating spring, axial spring, and shear spring, respectively, of the joints. Moreover, COMBIN14 is used to convey the forced displacement effect of the deformation in the foundation strata on the tunnel under earthquake conditions. The beam–spring model system formed is shown in Figure 10.

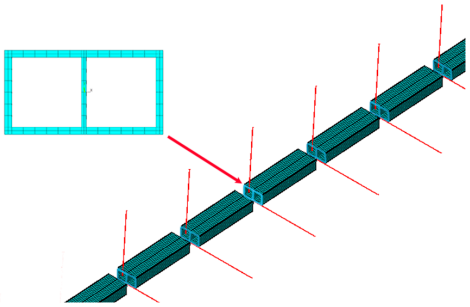

Figure 10. Longitudinal beam–spring model.

(3) Free-Field Analysis Model

The nonlinear material properties of soil are crucial in dynamic analysis. Consequently, a two-dimensional free-field model was established using the SuperFLUSH/2D program for equivalent linear analysis. The finite element model, depicted in Figure 11, incorporates viscous boundaries at the base and sides. Ground motion is introduced as an equivalent nodal force, enabling the determination of relative soil layer displacement along the immersed tunnel's entire domain through nonlinear seismic response analysis.

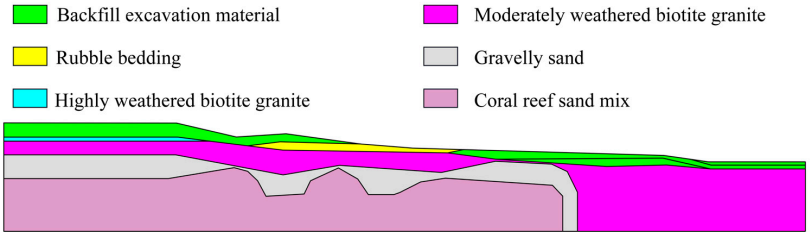

Figure 11. Longitudinal finite element model of the entire domain of immersed tunnel.

Relative displacement values of the surface, as well as the top and bottom of immersed tunnels under various ground motion conditions, are extracted and shown in Figure 12. These displacements are then applied to the ends of soil springs in the corresponding soil layers of the longitudinal beam–spring model. This approach allows for further analysis of the opening and relative angle of the immersed tunnel joints.

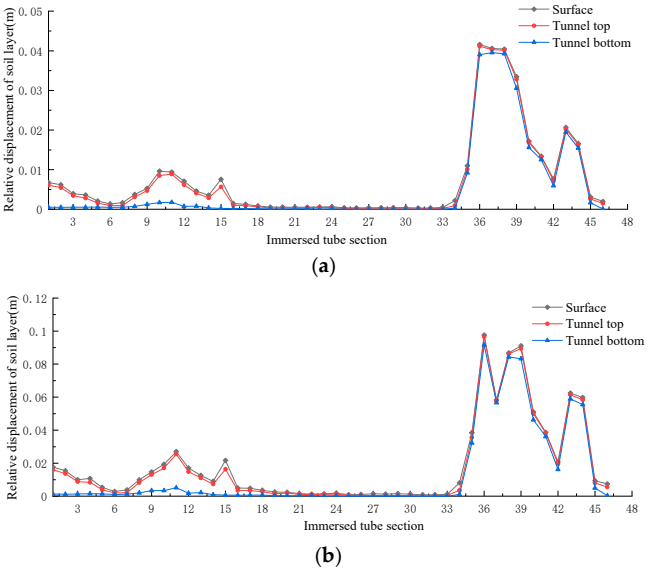

Figure 12. Relative displacement of soil layer in the entire domain of immersed tunnel: (**a**) working conditions under peak ground acceleration of 0.15 g; (**b**) working conditions under peak ground acceleration of 0.30 g.

3.2.2. Calculating Working Conditions

Investigations into nuclear power plant engineering reveal that the design value for the SL-2 level horizontal peak ground acceleration in China's coastal nuclear power plants typically ranges between 0.15 g and 0.30 g. For nuclear immersed tunnel conditions, it is essential to consider factors such as tunnel joint stiffness and varying peak ground accelerations. The seismic safety of immersed tunnels under diverse conditions must also be evaluated. This study simulates multiple scenarios to assess these aspects. Specifically, for the response displacement method in joint seismic performance analysis, peak accelerations of 0.15 g and 0.30 g and water stop stiffness values of 51 and 62 were selected, resulting in four distinct working conditions. Detailed information is presented in Table 2.

Table 2. Working conditions of calculation.

Peak Acceleration	Type of Water Stop	Joint Stiffness Coefficient				Working Condition
		Tensile Stiffness 10^6 (N·m^{-1})	Compressive Stiffness 10^6 (N·m^{-1})	Longitudinal Flexural Stiffness 10^9 (N·m^{-1}·rad)	Transverse Flexural Stiffness 10^{10} (N·m^{-1}·rad)	
0.15 g	320-370-51	150	1342	252	150	1
	320-370-62	207	1845	345	207	2
0.30 g	320-370-51	150	1342	252	150	3
	320-370-62	207	1845	345	207	4

3.2.3. Result Analysis

(1) Interlayer Displacement Angle

The interlayer displacement angle can be a good measure of the stability and damage degree of the structure under earthquake conditions. Table 3 summarizes the maximum interlayer displacement angles of the left wall, middle partition wall, and right wall under conditions 1 and 3. By analyzing these data, it is concluded that, under working condition 1, the largest angle is the right wall, with a maximum value of 1/7028; under working condition 3, the largest one is the right wall, with a maximum value of 1/7039. Both of these values are lower than the limit required by the "Standard for Seismic Design of Nuclear Power Plants".

Table 3. Interlayer displacement angle.

Working Condition	Peak Ground Acceleration	Left Side Wall	Middle Partition Wall	Right Side Wall	Code Limit Value
1	0.15 g	1/13745	1/9188	1/7028	1/550
3	0.30 g	1/10823	1/8428	1/7039	1/550

(2) Opening value of joints

For studying the change law in the longitudinal opening value of the immersed tunnel joint, the curves for each joint along the tunnel, depicting their positions under four different working conditions, are obtained. They are shown in Figure 13. It is found that all the parts with large joint openings are located in sections where there are changes in the thickness of the foundation strata and mutations in the soft and hard soil layers, while the parts with small opening values correspond to the positions where the thickness of the foundation strata is uniform.

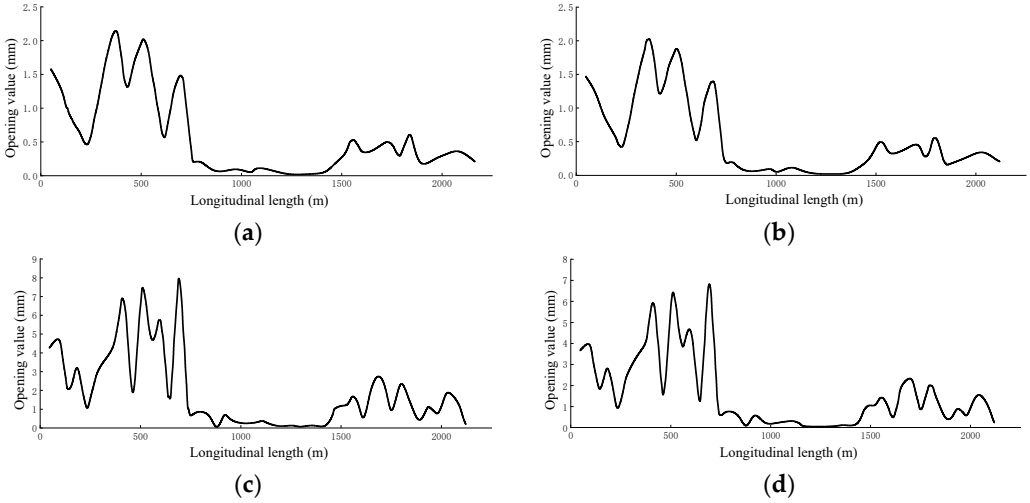

Figure 13. Distribution of joint opening values of immersed tunnel under different working conditions: (**a**) working condition 1, (**b**) working condition 2, (**c**) working condition 3, (**d**) working condition 4.

Compared with the change in the joint opening value under different working conditions, as the stiffness of the GINA waterproof strip increases, the longitudinal opening trend under different working conditions shows no significant changes with position, but the joint opening value decreases in all cases. For SL2 seismic peak accelerations of 0.15 g and 0.30 g, it was observed that the increase in seismic loading does not affect the trend of joint opening changes with position but results in an overall increase in joint opening.

3.3. Numerical Analysis Based on Dynamic Time-History Method

To conduct further research on the mechanical properties and seismic resistance of the immersed tunnel joints, based on the dynamic time-history method, the equivalent linear model and the viscoelastic boundary element are embedded in ANSYS by the subroutine of the UPFs, a secondary development program. Moreover, taking calculation time, calculation accuracy, storage cost, and other problems into consideration, a three-stage immersed tunnel with a relatively complex soil layer has been determined for modeling analysis. This study accurately simulates the tunnel joints and the effects of convection and impulse of the internal water flow, carrying out research on the interlayer displacement angle of the immersed tunnel, as well as the compression–tension variation and the opening value of its joints under ultimate seismic conditions. Lastly, the influence of joint stiffness on the seismic performance index has been analyzed.

3.3.1. Calculation Model

This study models three sections of an immersed tube, each 45 m in length, totaling 135 m. The immersed tunnels are simulated using eight-node shell elements (Shell281), GINA water stops with spring elements (Combine14), and soil and bedrock with eight-node solid elements (Solid181). Additionally, the convection and impulsive effects of moving water within the tunnel are modeled using mass point elements (Mass21) and spring elements (Combine14). This creates a comprehensive three-dimensional finite element model of the tunnel–joint–soil system. A viscoelastic boundary is set at the model's bottom and sides to simulate the radiation damping effect of an infinite foundation. The equivalent linear constitutive method describes the nonlinear characteristics of the soil mass. The soil layer model extends 50 m to both sides and 50 m below the tunnel center, with the tunnel buried at a depth of 13.2 m. The soil layers from top to bottom consist of coral reef mixed sand, medium sand, gravel cushion, highly weathered biotite granite, and moderately weathered biotite granite. In the mesh generation of the model, several key considerations are necessary. First, the balance between calculation cost and accuracy must

be maintained. The mesh size should be controlled, adhering to the "Standard for Seismic Design of Nuclear Power Plants" for maximum mesh size in the foundation strata. The immersed tunnels, being central to this research, should have a mesh size between 0.2 and 2 m, as illustrated in Figure 14. For the foundation, the mesh height of soil near the tunnel should match that of the immersed pipe as closely as possible, while the mesh height of soil farther from the tunnel can be increased, with a maximum of 5 m. The overall finite element model is shown in Figure 15. The first joint of the tunnel is located in a highly weathered soil layer and a gravel sand layer, both relatively thick, resulting in weaker bearing capacity compared to the second joint.

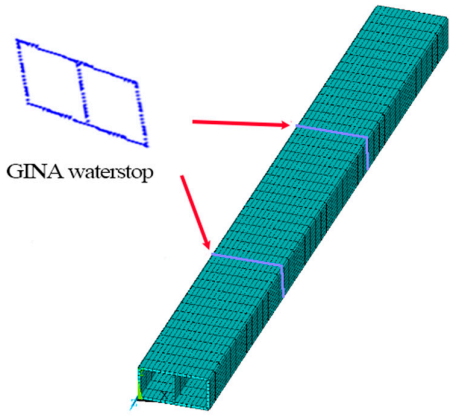

Figure 14. Immersed tunnel model and spring model.

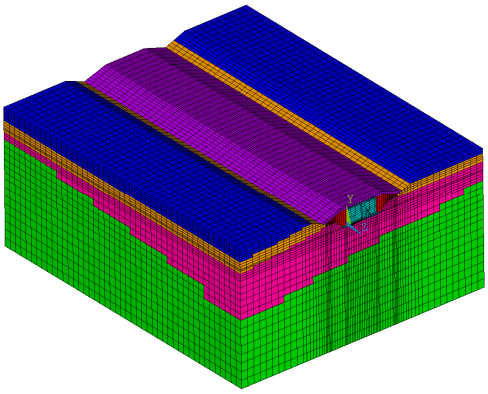

Figure 15. Immersed tunnel–joint–soil finite element model.

For convenience of expression, this paper has named the three sections of the immersed tube as follows: immersed tube No. 1, immersed tube No. 2, and immersed tube No. 3. Identically, the joints from left to right are named as follows: joint No. 1 and joint No. 2, which can be seen in Figure 16. Also, the walls of the immersed tunnel are named as follows: bottom plate 1, bottom plate 2, top plate 3, top plate 4, left side wall 5, middle partition wall 6, and right side wall 7, as shown in Figure 17.

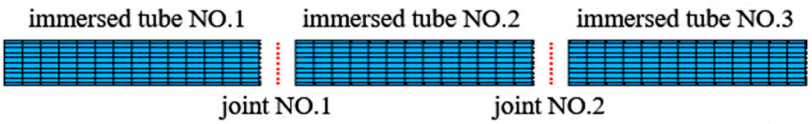

Figure 16. Numbers of each section of immersed tunnel.

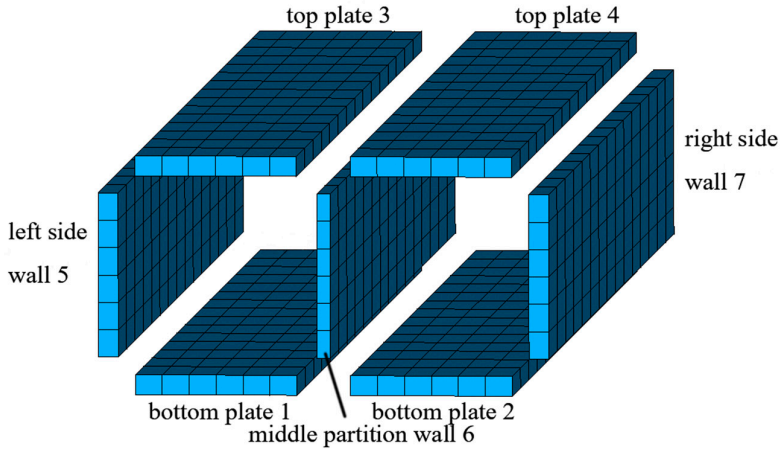

Figure 17. Locations of each wall of immersed tunnel.

3.3.2. Calculated Working Conditions

In this paper, a seismic load with a peak ground acceleration of 0.3 g is adopted to calculate the seismic response during the tunnel operating period. Additionally, hydrostatic pressure and hydrodynamic pressure, as well as high water levels, are taken into account. In addition, the combination of the action effects of the above loads is carried out according to the Code for Hydraulic Design of Nuclear Power Plants [32]. The joint GINA water stop is key to this study. Therefore, four water stops with different stiffness values and four working conditions are used in the calculation. The specific parameters of each condition are displayed in Table 4.

Table 4. Working conditions of calculation of seismic performance of immersed tunnel joints.

Peak Ground Acceleration	Type of Water Stop	Joint Stiffness Coefficient				Working Condition
		Tensile Stiffness 10^6 (N/m)	Compressive Stiffness 10^6 (N/m)	Longitudinal Flexural Stiffness 10^{11} (N/m·rad)	Transverse Flexural Stiffness 10^{10} (N/m·rad)	
SL2-0.3 g	320-370-51	150	1342	2.52	150	1
	320-370-62	207	1845	3.45	207	2

3.3.3. Analysis of Results

(1) Interlayer Displacement Angle

The interlayer displacement angles under dynamic and static conditions are superimposed, and the calculation results are shown in Table 5. From the table, the maximum displacement angle is 1/9429. Moreover, within the scope of the standard requirements, the interlayer displacement angle of the middle partition wall is always greater than that of the left and right side walls. From working condition 1 to 2, the stiffness of the joint water stop gradually increases while its interlayer displacement angle is gradually reduced, indicating that the interlayer displacement angle of the joint decreases with the increase in joint stiffness.

(2) Opening Value of Joints

Joints No. 1 and No. 2 of the immersed tunnel are located on a soil layer of varying thickness, so that the opening limits of the two joints are different under the same peak ground acceleration with identical stiffness. It can be seen from Figures 18 and 19 that the opening values of joints No. 1 and No. 2 under the two working conditions show a similar trend over time. The opening value is larger between 5 and 13 s, during which its changing value is more obvious. Hence, it can have a relatively serious impact on the joint water stop, which easily leads to the weakening of the water tightness of the immersed tunnel.

Table 5. Interlayer displacement angle under different working conditions.

Working Condition	Joint No. 1			Joint No. 2			Code Limit Value
	Left Side Wall 5	Middle Partition Wall 6	Right Side Wall 7	Left Side Wall 5	Middle Partition Wall 6	Right Side Wall 7	
Working condition 1	1/11579	1/10154	1/11000	1/10645	1/9429	1/10233	1/550
Working condition 2	1/15349	1/12692	1/14043	1/13469	1/11786	1/13018	

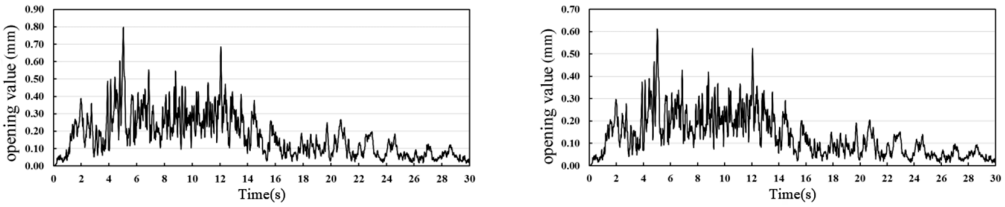

(**a**) (**b**)

Figure 18. Opening values of joint No. 1: (**a**) opening value under working condition 1; (**b**) opening value under working condition 2.

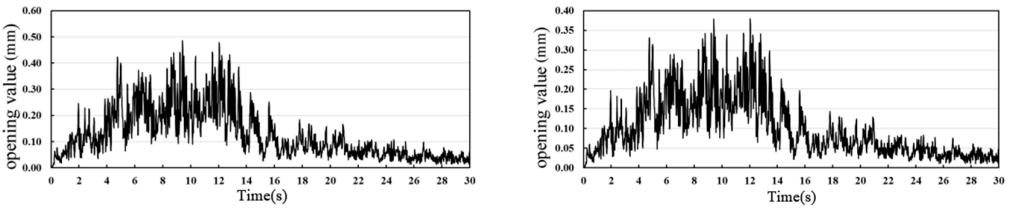

(**a**) (**b**)

Figure 19. Opening values of joint No. 2: (**a**) opening value under working condition 1; (**b**) opening value under working condition 2.

After the superposition of dynamic and static working conditions, the comprehensive opening value is obtained. Under working condition 1, the maximum opening value of joint No. 1 is 0.85 mm, while that of joint No. 2 is 0.49 mm. Under working condition 2, the former is 0.66 mm, while the latter is 0.38 mm. On the whole, the opening value under the dynamic condition is the main influencing factor, with that under the static condition having less effect. The opening values of joint water stops No. 1 and No. 2 under each working condition is shown in Table 6.

Table 6. Maximum opening value of joints under each working condition (unit: mm).

Joint	Working Condition	Type of Water Stop	Maximum Opening Value under Dynamic Condition	Maximum Opening Value under Static Condition	Comprehensive Opening Value
Joint No. 1	Condition 1	51	0.797	0.0496	0.8466
	Condition 2	62	0.611	0.0496	0.6606
Joint No. 2	Condition 1	51	0.486	0.0014	0.4874
	Condition 2	62	0.379	0.0014	0.3804

(3) Compression–Tension Value and Sensitivity Analysis of GINA Water Stop

The compression and tension values of GINA water stops at each joint are shown in Figures 20 and 21. Positive values indicate tension, while negative values indicate

compression. An analysis of the change curves for joints No. 1 and No. 2 under the two working conditions reveals that joint No. 1 experiences the largest compression and tension, with maximum compression values of 0.55 mm and 0.73 mm and maximum tension values of 0.41 mm and 0.54 mm. Additionally, from working condition 1 to 2, the maximum compression values for joints No. 1 and 2 decrease sequentially, and their tension values significantly exceed their compression ones. This is attributed to the compressive stiffness of the joint water stop being greater than its tensile stiffness.

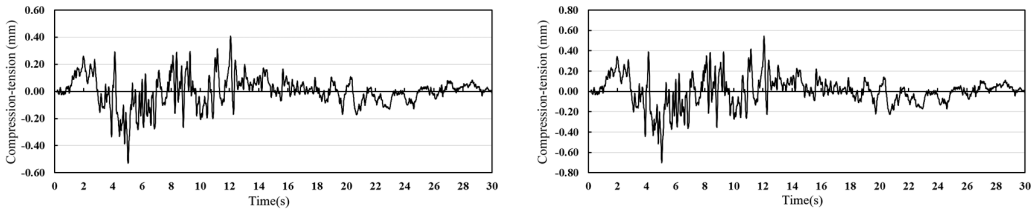

Figure 20. Compression–tension values of joint No. 1: (**a**) compression–tension value under working condition 1; (**b**) compression–tension value under working condition 2.

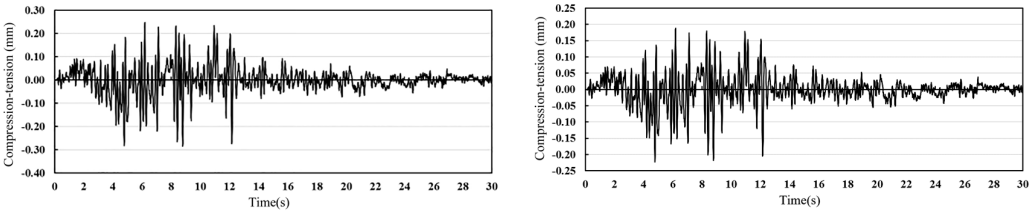

Figure 21. Compression–tension values of joint No. 2: (**a**) compression–tension value under working condition 1; (**b**) compression–tension value under working condition 2.

So as to deeply analyze the response rule of the joint water stop of an immersed tunnel under seismic conditions, this paper also sets up two different water stop stiffness values as working conditions for calculation and discusses the impact of the different stiffness values of the GINA water stop on the compression and tension values of the immersed tunnel.

Figure 22 depicts the changes in the compressive stiffness of the maximum compression–tension values of the joint water stop under a peak ground acceleration of 0.3 g. When the compressive stiffness value of both joint No. 1 and joint 2 is 819 × 106 N/m, the maximum tension of joint No. 1 is far greater than that of joint No. 2. When the tensile stiffness is 92 × 106 N/m for both joints, the maximum tension value of joint No. 1 is also much greater than that of joint No. 2, which denotes that the thickness of the highly weathered biotite granite and medium-weathered biotite granite on the foundation where joints No. 1 and No. 2 are located has a large bearing on the maximum compression–tension value of the joint. Furthermore, with the increase in compressive and tensile stiffness of the GINA water stop, its maximum compression–tension value gradually decreases, the speed of which progressively slows down. Lastly, the maximum tension value of joint No. 1 is significantly greater than that of joint No. 2, implying that as the compressive and tensile stiffness values increase to a certain extent, the influence of the change in stiffness value on the value of the maximum tension of the joint gradually declines.

It is also worth noticing that there is no definite value for the ultimate compression–tension value of the immersed tunnel's joint stop belt by now, which mainly depends on factors including joint structure, the material of the water stop, construction errors, and so on. At present, among the seismic codes of underground engineering structures, only the "Code for Seismic Design of Highway Tunnel" [33] has made corresponding provisions on joint opening values for immersed tunnels, stipulating that the opening value should not

exceed 40 mm under E2 earthquake conditions. Accordingly, the seismic calculation of the opening values in this paper is within the allowable range.

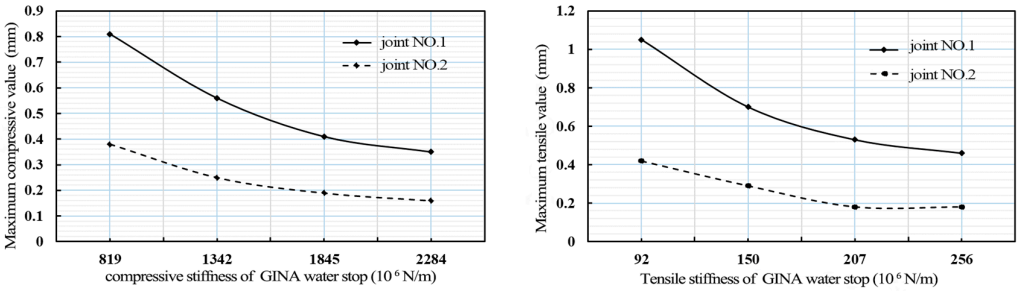

(**a**) (**b**)

Figure 22. Relationship between the stiffness of GINA water stop and the maximum compression–tension value: (**a**) maximum compression value; (**b**) maximum tension value.

4. Conclusions

In this paper, the beam–spring model and the shield tunnel–foundation three-dimensional finite element model is established based on the water-intake project of an immersed tunnel in a nuclear power sea area. Additionally, we implemented secondary development in ANSYS to create equivalent linear dynamic constitutive and viscoelastic boundary element subroutines. Our research focused on the seismic performance of the immersed tunnel under ultimate seismic ground motion (SL-2), with particular attention to the seismic analysis of the tunnel joints. The primary findings are as follows:

(1) Using the response displacement method, we found that increases in joint stiffness and peak ground acceleration do not affect the variation trend of joint openings along the longitudinal position of the immersed tunnel. However, significant changes in joint openings are observed at locations where the overburden thickness changes abruptly or where there is an uneven distribution of soft and hard soil. Additionally, higher stiffness of the joint GINA water stop results in a smaller maximum opening value and a reduced maximum relative angle of the joint.

(2) Variations in soil thickness on either side of the foundation and tunnels significantly impact the maximum compression–tension value of the immersed tunnel joint water stop. As the stiffness of the GINA water stop increases, the compression–tension value gradually decreases, with diminishing reductions at higher stiffness levels. When the stiffness exceeds a certain threshold, its influence on the compression–tension value weakens.

(3) The deformation of the immersed tunnel is influenced by the surrounding soil layer's deformation. To mitigate forced displacement of the relatively rigid immersed tunnel due to uneven geological conditions, especially the adverse effects of ground motion, flexible joint structural measures should be adopted based on the actual foundation conditions. Additionally, it is essential to fully mobilize the supporting forces of the surrounding rocks to accommodate uneven soil layer deformation during earthquakes.

(4) The analysis results indicate that time-history analysis provides relatively quantitative and accurate results for seismic response analysis of structures such as immersed tunnels. Qualitative analyses can also be performed using the response displacement method in practical applications. Future research should focus on developing calculation programs for the generalized response displacement method.

Author Contributions: Resources, J.Z.; project administration, J.Z.; funding acquisition, J.Z.; methodology, J.Z., B.Q. and C.G.; conceptualization, J.Z., B.Q. and C.G.; writing—original draft, B.Q.; writing—review and editing, J.Z., B.Q., J.W. and Y.P.; software, C.G.; data curation, C.G.; visualization, J.W. and Y.P. All authors have read and agreed to the published version of the manuscript.

Funding: Key Project of the National Natural Science Foundation of China [51738010] and Dalian Science and Technology Innovation Fund Project [2021JJ13SN83].

Institutional Review Board Statement: Not applicable.

Informed Consent Statement: Not applicable.

Data Availability Statement: The raw data supporting the conclusions of this article will be made available by the authors on request.

Conflicts of Interest: Author Changjiang Gan was employed by the company Gansu Comprehensive Railway Engineering Contracting Co., Ltd. The remaining authors declare that the research was conducted in the absence of any commercial or financial relationships that could be construed as a potential conflict of interest.

References

1. Yan, W.; Xie, Z.; Zhang, X.; Wang, J.; Gao, X. Tests for compartmental particle damper's a seismic control in an immersed tunnel. *J. Vib. Shock* **2016**, *35*, 7–12.
2. Cheng, X.; Jing, L.; Cui, J.; Li, Y.; Dong, R. Research of shaking table model tests on immersed tunnels under different conditions. *J. Southwest Jiaotong Univ.* **2017**, *52*, 1113–1120.
3. Zhang, X.; Yan, W.; Chen, Y.; Chen, S.C.; Chen, H.J. Shaking tables tests for an immersed tunnel model considering wave passage effect. *J. Vib. Shock.* **2018**, *37*, 76–84.
4. Yuan, Y.; Yu, H.; Xiao, W.; Xu, G.; Ji, Z. Experimental failure analysis on concrete shear keys in immersion joint subjected to compression-shear loading. *Eng. Mech.* **2017**, *34*, 149–181.
5. Okamoto, S.; Tamura, C. Behaviour of Subaqueous Tunnels During Earthquakes. *Earthq. Eng. Struct. Dyn.* **1973**, *1*, 253–266. [CrossRef]
6. Chen, H.-J. Theoretical Analysis and Experimental Research on Seismic Performance of Immersed Tunnel and Its Joints. Ph.D. Thesis, Beijing University of Technology, Beijing, China, 2014.
7. Li, Y.; Tian, Y.; Zong, J. Shaking table test of a tunnel-soil system considering the influence of surface buildings under multi-dimensional seismic waves. *Chin. J. Rock Mech. Eng.* **2022**, *41*, 1453–1465.
8. Li, Y.; Tian, Y.; Zong, J. Shaking table test of soil and tunnel considering surface construction under multi-dimensional earthquake. *Chin. J. Rock Mech. Eng.* **2022**, *41*, 1–13.
9. Peng, H.; Meng, G.; Ding, Q.; Xu, F. The influence of hydrodynamic pressure on immersed tunnel under earthquake excitation. *J. Shanghai Jiaotong Univ.* **2008**, 1027–1031. [CrossRef]
10. Chen, W.; Lv, Z.; Xu, L.; Ruan, B.; Ma, J.; Chen, X. Seismic response of subsea tunnels considering seawater seabed coupling effect. *J. Eng. Geol.* **2021**, *29*, 1878–1886. [CrossRef]
11. Cui, J.; Zhou, P.; Li, Y.; Ouyang, Z. Earthquake dynamic response analysis of seabed under the action of immersed tunnel. *Earthq. Eng. Eng. Dyn.* **2016**, *4*, 96–102. [CrossRef]
12. Xiao, W.; Chai, R.; Yu, H.; Yuan, Y. Simulation method for nonlinear mechanical properties of immersed tunnel joint. *Mech. Eng.* **2014**, *36*, 757–763.
13. Zhang, X.; Zhao, G.; Ye, G.; Wang, J. Simplified method and three-dimensional finite element analysis of quake-proof for immersed tunnel joints. *Chin. J. Undergr. Space Eng.* **2011**, *7*, 1292–1297+1402.
14. Yu, H.; Song, Y.; Li, Y.; Zhang, S.; Xu, L. Multi-scale method and seismic response analysis of immersed tunnel. *J. Tongji Univ. Nat. Sci.* **2021**, *49*, 807–815.
15. He, C.; Xu, G.; Zhang, Z. Mechanical properties of shear keys of segment joints in immersed tunnels under seismic loading. *J. Northeast. Univ. Nat. Sci.* **2021**, *42*, 871–878.
16. Cui, J.; Lu, Y.; Qu, J.; Li, Y. Analysis of the Affecting Factors for Seismic Response of Immersed Tunnel. *J. Southwest Jiaotong Univ.* **2020**, *55*, 1224–1230.
17. Bai, L.; Zhao, X.; Du, X.; Yuan, Y.; Liu, H. Seismic Response of Joints of Immersed Tunnels. *J. Disaster Prev. Mitig. Eng.* **2015**, *35*, 153–159+165. [CrossRef]
18. Hu, Z. *Research on Action Mechanisms and Structural Properties of Segmental Joint Shear Keys on Immersed Tunnel*; Chang'an University: Xi'an, China, 2015.
19. Lin, W.; Liu, X. Analysis of GINA uneven compression during hydraulic connection of immersed tunnel element at curved plane design line. *China Harb. Constr.* **2016**, *36*, 51–53.
20. Liu, Y.; Wang, X.; Xu, Y. Technology for installation of GINA gasket. *China Harb. Eng.* **2016**, *36*, 66–68.
21. Bai, Y.; Lu, H. Damage Analysis and Repair Technology of OMEGA Gasket in Immersed Tunnel. *J. Railw. Eng. Soc.* **2016**, *33*, 87–92.
22. Chen, Y.; Zhang, B.; Wang, S.; Liu, Q.; Song, C. Research status and Engineering application of rubber water stop for immersed tunnel. *Spec. Purp. Rubber Prod.* **2012**, *33*, 60–64.
23. Zhang, W.; Yan, H. Development of New type Omega rubber water stop. *Spec. Purp. Rubber Prod.* **2014**, *35*, 50–52.
24. Liu, Z.; Huang, H. Performance Evaluation and Safety Pre-warning of GINA in Immersed Tube Tunnel. *Chin. J. Undergr. Space Eng.* **2009**, *5*, 347–353.

25. Zhang, Y.; Wang, H.; Guo, J.; Deng, X.; Luo, J. Vertical Compression Shear Mechanical Performance Study of Immersed Tunnel Joint. *Chin. J. Undergr. Space Eng.* **2016**, *12*, 24–31.
26. Wang, X. *ANASYS Structure Analysis and Application*; China Communication Press: Beijing, China, 2011.
27. *GB 50267-2019*; Standard for Seismic Design of Nuclear Power Plants. China Planning Press: Beijing, China, 2019.
28. *ASCE 4-98-2000*; Seismic Analysis of Safety-Related Nuclear Structures and Commentary. American Society of Civil Engineers: Reston, VA, USA, 2000.
29. Cao, J.; Tao, G.; Deng, Y. Research on dynamic response of ship cabin structure based on modified Housner model. *Water Transp. Eng.* **2021**, 117–122+155.
30. Guan, Q.; Fei, W.; Liu, J. Secondary development and application of equivalent linear viscoelastic model based on ANSYS. *Water Resour. Power* **2022**, *40*, 100–104.
31. Ma, S.; Chi, M.; Chen, H.; Chen, S. Implementation of viscoelastic artificial boundary in ABAQUS and comparative study of seismic input methods. *Chin. J. Rock Mech. Eng.* **2020**, *39*, 1445–1457.
32. *NB/T 25046-2015*; Code for Hydraulic Design of Nuclear Power Plants. China Planning Press: Beijing, China, 2015.
33. *JTGT 2232-2019*; Specifications for Seismic Design of Highway Tunnels. China Communication Press: Beijing, China, 2019.